Energy Trading and Time Scheduling for Energy-Efficient Heterogeneous Low-Power IoT Networks

Ngoc-Tan Nguyen[12], Diep N. Nguyen[1], Dinh Thai Hoang[1], Nguyen Van Huynh[1],
Hoang-Nam Nguyen[2], Quoc Tuan Nguyen[2], and Eryk Dutkiewicz[1]
[1] School of Electrical and Data Engineering, University of Technology Sydney, Australia
[2] JTIRC, VNU University of Engineering and Technology, Vietnam National University, Hanoi, Vietnam

***Abstract*—In this paper, an economic model is proposed to jointly optimize profits for participants in a heterogeneous IoT wireless-powered backscatter communication network. In the network under considerations, a power beacon and IoT devices (with various communication types and energy constraints) are assumed to belong to different service providers, i.e., energy service provider (ESP) and IoT service provider (ISP), respectively. To jointly maximize the utility for both service providers in terms of energy efficiency and network throughput, a Stackelberg game model is proposed to study the strategic interaction between the ISP and ESP. In particular, the ISP first evaluates its benefits from providing IoT services to its customers and then sends its requested price together with the service time to the ESP. Based on the request from the ISP, the ESP offers an optimized transmission power that maximizes its utility while meeting energy demands of the ISP. To study the *Stackelberg equilibrium*, we first obtain a closed-form solution for the ESP and propose a low-complexity iterative method based on *block coordinate descent* (BCD) to address the non-convex optimization problem for the ISP. Through simulation results, we show that our approach can significantly improve the profits for both providers compared with those of conventional transmission methods, e.g., bistatic backscatter and harvest-then-transmit communication methods.**

***Index Terms*—Stackelberg game, bistatic backscatter, low-power communications, heterogeneous IoT networks.**

I. Introduction

Emerging Internet of Things (IoT) converges various technologies to connect diverse smart devices to the Internet and enables ubiquitous information/data collecting and sharing. Over the last decade, with rapid development, IoT has found its application in almost every corner of life, e.g., smart city, home, agriculture, healthcare, and transportation [1]. To meet low-cost and lightweight requirements, IoT devices are usually powered by batteries. However, regular battery recharging/replacing for a massive number of such IoT devices is ineffective because it is costly, inconvenient, and impractical in some cases (e.g., biomedical implants) [2]. The emerging wireless-powered backscatter communication (WPBC) can be a great potential solution to tackle this problem [3]-[5].

A WPBC network integrates two well-known technologies seamlessly, which are *Harvest-then-Transmit* (HTT) [6] and backscatter communications [7]. In a WPBC network, a wireless-powered device (WPD) can perform either backscatter communications (i.e., passive transmissions) or transmissions using its radio frequency (RF) circuit (i.e., active transmissions) and the energy harvested from a power beacon (PB).

Most existing work on the WPBC optimizes time allocation for devices to perform energy harvesting, active and passive transmissions under the time-division multiplexing (TDM) framework with the assumption of homogeneous IoT devices [3]-[5]. In practice, various types of WPDs with different hardware capabilities and configurations, e.g., performing backscattering or HTT or both can co-exist. Moreover, a large number of IoT devices can belong to an IoT service provider (ISP) who is required to pay for energy to operate its service (e.g., a contractor that provides data collecting/monitoring services for smart cities). In such a case, the energy cost/negotiation between the ISP and an energy service provider (ESP) should be taken into account while optimizing the scheduling of IoT devices.

Our work in this paper aims to address the above by studying the strategic interaction between the ISP and ESP (via the PB) and its implication on optimizing the energy trading and time scheduling for a heterogeneous WPBC (HWPBC) network. Specifically, we use the Stackelberg game to capture the strategic interaction between the PB and the IoT devices [4]-[5]. Under such a game, the ISP that acts as the leader can proactively select an energy service by sending its energy request with a price and charging time. It is due to the fact that an ISP has more than one option to select an ESP. Thus, it takes the advantage to initiate the game. The ESP modeled as the follower then finds the optimal transmission power which can maximize its benefits while meeting requirements from the ISP. A quadratic price model for energy trading [8] is developed to optimize the profit of the ESP, i.e., the follower, achieved by selling energy based on the requested price and operation time of the ISP, i.e., the leader. The profit of the ISP is the difference between the revenue from providing services (i.e., collecting data) and the energy cost. The maximization of the ISP's profit is a non-convex problem with respect to the requested price, and operation times of the PB and IoT devices. To maximize this profit, we propose an iterative algorithm developed based on the *block coordinate descent* (BCD) method [9]. As a result, our proposed approach can guarantee to always achieve the local *Stackelberg equilibrium* (SE). Numerical results then verify the efficiency of the proposed approach compared with other baseline methods (i.e., bistatic backscatter communication mode (BBCM) [10] and HTT communication mode (HTTCM) [6]).

II. System Model

A. Network Setting

As illustrated in Fig. 1(a), we consider the HWPBC consisting of two service providers, i.e., the ISP and ESP. At the ISP,

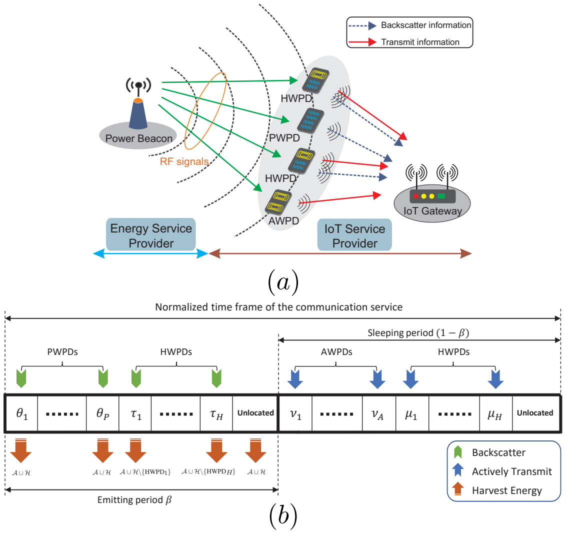

Fig. 1: (a) System model (b) Time frame for the IoT service.

we consider three types of low-cost IoT devices with dissimilar hardware configurations that can support two functions: i.e., the BBCM and/or HTTCM. The first set of IoT devices represented by $\mathcal{A} \triangleq \{\text{AWPD}_a | \forall a = \{1, \dots, A\}\}$ is active wireless-powered IoT devices (AWPDs) that are equipped with energy harvesting and wireless transmission circuits. With this configuration, the AWPDs can operate in the HTTCM only. In addition, we denote $\mathcal{P} \triangleq \{\text{PWPD}_p | \forall p = \{1, \dots, P\}\}$ to be the set of passive wireless-powered IoT devices (PWPDs) that are designed with a backscattering circuit to perform the BBCM only. Finally, hybrid wireless-powered IoT devices (HWPDs) belonging to the set $\mathcal{H} \triangleq \{\text{HWPD}_h | \forall h = \{1, \dots, H\}\}$ are equipped with all hardware components to support both aforementioned operation modes. On the other hand, the ESP utilizes a dedicated PB to supply energy for the IoT devices.

The IoT service is operated over two consecutive working periods of the PB, i.e., *emitting period* β and *sleeping period* $(1-\beta)$ as shown in Fig. 1(b). For simplicity and efficiency in time resource allocation for multiple IoT devices, the TDM framework is adopted here to avoid collisions among transmissions. We denote $\boldsymbol{\theta} \triangleq (\theta_1, \dots, \theta_p, \dots, \theta_P)^{\mathrm{T}}$ and $\boldsymbol{\tau} \triangleq (\tau_1, \dots, \tau_h, \dots, \tau_H)^{\mathrm{T}}$ as the backscattering time vectors for the PWPDs and HWPDs in the emitting period of the PB, respectively. Similarly, $\boldsymbol{\nu} \triangleq (\nu_1, \dots, \nu_a, \dots, \nu_A)^{\mathrm{T}}$ and $\boldsymbol{\mu} \triangleq (\mu_1, \dots, \mu_h, \dots, \mu_H)^{\mathrm{T}}$ are the transmission time vectors for AWPDs and HWPDs in the idle period of the PB, respectively. When the PB is in the emitting period, it transmits unmodulated RF signals, and thus the IoT devices (i.e., PWPDs and HWPDs) with the capability of backscattering can passively transmit their data by leveraging such signals. Meanwhile, the AWPDs and HWPDs equipped with energy harvesting circuits can harvest energy for their active transmissions in the sleeping period of the PB. Note that, an AWPD_a can execute energy harvesting in the entire emitting period (i.e., β), while the harvesting time of an HWPD_h is $(\beta - \tau_h)$ because it must backscatter in the time slot τ_h. In the sleeping period of the PB, the AWPDs and HWPDs can perform active transmissions to deliver their data to the gateway based on the TDMA protocol.

B. Network Throughput Analysis

1) Emitting period of the PB: Assume that the achievable backscatter rates (in bits/s) of the PWPD_p and HWPD_h are W_p and W_h, respectively. The total throughput obtained by backscatter communications in the emitting period of the PB is $R^{bb} = \sum_{p=1}^{P} \gamma_p W_p \theta_p + \sum_{h=1}^{H} \gamma_h W_h \tau_h$, where γ_p and γ_h are the backscattering efficiency coefficients [10] of the PWPD_p and HWPD_h, respectively.

2) Sleeping period of the PB: As mentioned in the previous subsection, only AWPDs and HWPDs are able to communicate with the gateway in this period by using their RF transmission circuits. The amount of harvested energy of the AWPD_a and HWPD_h from the PB are calculated as follows:

$$\begin{cases} E_a = \beta P_a^R, \\ E_h = (\beta - \tau_h) P_h^R, \end{cases} \tag{1}$$

where $P_a^R = \varphi_a P_S \frac{G^T G_a^R \lambda^2}{(4\pi d_a)^2}$ and $P_h^R = \varphi_h P_S \frac{G^T G_h^R \lambda^2}{(4\pi d_h)^2}$ are the received power at the AWPD_a and HWPD_h, respectively [11]. P_S and G^T are the transmission power and antenna gain of the energy transmitter (i.e., the PB), respectively. $\{\varphi_a, \varphi_h\}$ and $\{G_a^R, G_h^R\}$ are the harvesting efficiency coefficients and antenna gains of the AWPD_a and HWPD_h, respectively. λ is the wavelength of the RF signal, d_a and d_h are the distances from the PB to the AWPD_a and HWPD_h, respectively. We consider the energy consumption by active transmissions of the AWPDs and HWPDs as the dominant energy consumption and ignore the energy consumed by electronic circuits. Hence, all harvested energy of the AWPDs and HWPDs is utilized to transmit data in the sleeping period of the PB, and the transmission power of the AWPD_a and HWPD_h are $P_a^t = E_a/\nu_a$ and $P_h^t = E_h/\mu_h$, respectively. Then, the total throughput R^{st} achieved by active transmissions of the AWPDs and HWPDs in the sleeping period of the PB is determined by:

$$\begin{aligned} R^{st} &= \sum_{a=1}^{A} \nu_a \phi_a \Omega \log_2\left(1 + \rho_a \frac{P_a^t}{N_a^0}\right) + \sum_{h=1}^{H} \mu_h \phi_h \Omega \log_2\left(1 + \rho_h \frac{P_h^t}{N_h^0}\right) \\ &= \sum_{a=1}^{A} \nu_a \kappa_a \log_2\left(1 + \delta_a \frac{\beta P_S}{\nu_a}\right) + \sum_{h=1}^{H} \mu_h \kappa_h \log_2\left[1 + \delta_h \frac{(\beta - \tau_h) P_S}{\mu_h}\right], \end{aligned} \tag{2}$$

where $\kappa_a = \phi_a \Omega$, $\kappa_h = \phi_h \Omega$, $\eta_a = \rho_a / N_a^0$, $\eta_h = \rho_h / N_h^0$, $\delta_a = \eta_a \varphi_a \frac{G^T G_a^R \lambda^2}{(4\pi d_a)^2}$ and $\delta_h = \eta_h \varphi_h \frac{G^T G_h^R \lambda^2}{(4\pi d_h)^2}$. $\{\phi_a, \phi_h\} \in (0, 1)$ are the transmission efficiency coefficients of the AWPD_a and HWPD_h, respectively. Ω is the bandwidth, $\{\rho_a, \rho_h\}$ and $\{N_a^0, N_h^0\}$ are the channel gains and White noise of the communication channels from the AWPD_a and HWPD_h to the gateway, respectively.

Finally, the network throughput (R_{sum}) can be determined as in (3) and modeled as the achieved profit of the ISP to jointly maximize the benefits of both service providers.

$$\begin{aligned} R_{sum}(\boldsymbol{\theta}, \boldsymbol{\nu}, \boldsymbol{\tau}, \boldsymbol{\mu}) &= R^{bb} + R^{st} \\ &= \sum_{p=1}^{P} \gamma_p \mathrm{W}_p \theta_p + \sum_{a=1}^{A} \nu_a \kappa_a \log_2\left(1 + \delta_a \frac{\beta P_S}{\nu_a}\right) \\ &\quad + \sum_{h=1}^{H} \left\{ \gamma_h \mathrm{W}_h \tau_h + \mu_h \kappa_h \log_2\left[1 + \delta_h \frac{(\beta - \tau_h) P_S}{\mu_h}\right] \right\}. \end{aligned} \tag{3}$$

III. Joint Energy Trading and Time Scheduling based on Stackelberg Game

A. Game Formulation

1) Leader payoff function: The achievable benefit of the ISP is defined as follows:

$$\boldsymbol{U}_L(p_l, \beta, \boldsymbol{\psi}) = p_r R_{sum} - p_l \beta P_S, \tag{4}$$

where p_r is the benefit per bit transmitted by IoT devices, and p_l is the energy price paid by the ISP to the ESP. The leader maximizes its utility function U_L w.r.t. the energy price p_l, operation time β, and time scheduling $\boldsymbol{\psi} \triangleq (\boldsymbol{\theta}, \boldsymbol{\nu}, \boldsymbol{\tau}, \boldsymbol{\mu})$.

2) Follower utility function: In this game, the PB is the follower and it optimizes its transmission power based on the requested energy price and operation time from the ISP. The utility function of the follower is determined based on its profit obtained from the ISP and its cost incurred during the operation time:

$$\boldsymbol{U}_F(P_S) = \beta \left[\, p_l P_S - F(P_S) \right], \tag{5}$$

where $F(x) = a_m x^2 + b_m x$ is a quadratic function which is applied for the operation cost of the PB [8].

B. Solution to the Stackelberg Game

The definition of the Stackelberg equilibrium (SE) is stated below.

Definition 1. *The optimal solution* $(P_S^*, p_l^*, \beta^*, \boldsymbol{\psi}^*)$ *is the SE if the following conditions are satisfied* [12]*:*

$$\begin{cases} \boldsymbol{U}_L(P_S^*, p_l^*, \beta^*, \boldsymbol{\psi}^*) \geq \boldsymbol{U}_L(P_S^*, p_l, \beta, \boldsymbol{\psi})\,, \\ \boldsymbol{U}_F(P_S^*, p_l^*, \beta^*, \boldsymbol{\psi}^*) \geq \boldsymbol{U}_F(P_S, p_l^*, \beta^*, \boldsymbol{\psi}^*)\,. \end{cases} \tag{6}$$

We adopt the backward induction technique to obtain the Stackelberg game solution. Firstly, given a strategy of the leader (i.e., ISP), the follower (i.e., ESP) can obtain a unique optimal closed-form solution $P_S^* = \frac{p_l - b_m}{2a_m}$ since the follower's utility is a quadratic function. Then, given the optimal transmission power P_S^* of the ESP, the leader payoff function can be rewritten in (7). Then, the maximum profit of the leader is expressed as follows:

$$\max_{(p_l, \beta, \boldsymbol{\psi})} \boldsymbol{U}_L(p_l, \beta, \boldsymbol{\psi})\,, \tag{8}$$

$$\text{s.t. } 0 \leq P_S \leq P_S^{max}, \tag{8a}$$

$$\beta P_a^R \leq \nu_a P_a^{\max}, \tag{8b}$$

$$(\beta - \tau_h)\, P_h^R \leq \mu_h P_h^{\max}, \tag{8c}$$

$$E_a^{min} \leq \beta P_a^R \leq E_a^{max}, \tag{8d}$$

$$E_h^{min} \leq (\beta - \tau_h) P_h^R \leq E_h^{max}, \tag{8e}$$

$$0 \leq \sum\nolimits_{p=1}^{P} \theta_p + \sum\nolimits_{h=1}^{H} \tau_h \leq \beta \leq 1, \forall \theta_p, \forall \tau_h \geq 0, \tag{8f}$$

$$0 \leq \sum\nolimits_{a=1}^{A} \nu_a + \sum\nolimits_{h=1}^{H} \mu_h \leq 1 - \beta \leq 1, \forall \nu_a, \forall \mu_h \geq 0, \tag{8g}$$

where $P_S = \frac{(p_l - b_m)}{2a_m}, P_a^R = \frac{\delta_a (p_l - b_m)}{2\eta_a a_m}, P_h^R = \frac{\delta_h (p_l - b_m)}{2\eta_h a_m}$. Firstly, the transmission power of the PB must satisfy the FCC Rules [13] as shown in the constraint (8a). For the IoT devices, the transmission power of AWPDs and HWPDs must follow the constraints (8b)-(8c). Moreover, the total energy harvested by the AWPDs and HWPDs must also satisfy the constraints (8d)-(8e). Finally, the constraints (8f)-(8g) are time constraints for IoT devices.

However, the problem (8) is a non-concave problem due to its non-convex constraints (8d)-(8d). Note that the game with non-concave utility-maximization problem is often referred to as non-convex or non-concave game that is challenging. In this case, one tends to relax the equilibrium concept to quasi-equilibrium [14]-[16]. In our case, a quasi-SE (QSE) can be defined as a solution of a variational inequality [17] equivalent-problem obtained under the *Karush–Kuhn–Tucker* (K.K.T.) optimality conditions of the non-cave problem. However, in our work, we adopt the concept of local SE that is defined as follows [18]-[19]:

Definition 2. *Let* $\boldsymbol{\chi} \triangleq (p_l, \beta, \boldsymbol{\psi})$ *be the variable tuple of the problem* (8) *and* $S_{\boldsymbol{\chi}}$ *be the constraint set determined by the constraints* (8a)-(8f)*. A pair* $(P_S^*, \hat{\boldsymbol{\chi}}^*)$ *is a local SE of the proposed Stackelberg game if there exists a neighborhood* $\hat{S}_{\boldsymbol{\chi}}$ *around* $\hat{\boldsymbol{\chi}}^*$ *so that for all* $\boldsymbol{\chi} \in \hat{S}_{\boldsymbol{\chi}} \subset S_{\boldsymbol{\chi}}$*, we have:*

$$\boldsymbol{U}_L\left(\hat{\boldsymbol{\chi}}^*, P_S^*\right) \geq \boldsymbol{U}_L\left(\boldsymbol{\chi}, P_S^*\right). \tag{9}$$

IV. Iterative Algorithm to Find the Local Stackelberg Equilibrium

To address the non-convex optimization problem (8), we propose an iterative algorithm exploiting the BCD technique to divide the variable tuple $\boldsymbol{\chi}$ into 3 different blocks of variables, i.e., the energy price p_l, the emitting time β, and the scheduling times $\boldsymbol{\psi}$. In particular, the algorithm starts by initializing an initial solution $\{{p_l}^{(0)}, \beta^{(0)}, \boldsymbol{\psi}^{(0)}\}$. The following three steps are repeated until convergence: (i) optimize the energy price ${p_l}^{(n)}$ from the last optimal output $\{p_l^{(n-1)}, \beta^{(n-1)}, \boldsymbol{\psi}^{(n-1)}\}$; (ii) obtain the emitting time of the PB $\beta^{(n)}$ by keeping the $\{{p_l}^{(n)}, \boldsymbol{\psi}^{(n-1)}\}$ fixed; (iii) find the optimal scheduling times $\boldsymbol{\psi}^{(n)}$ of the IoT devices with the fixed ${p_l}^{(n)}$ and $\beta^{(n)}$. These sub-problems are then proved to be convex and solved in sequence at each loop.

A. Optimal Energy Price Offered for the PB

In this subsection, we first obtain the optimal requested price p_l based on the optimal solution from the previous step $\{p_l^{(n-1)}, \beta^{(n-1)}, \boldsymbol{\psi}^{(n-1)}\}$. Note that, the time constraints in the problem (8) are eliminated because the time variables are constant and set by the previous optimal vector $\boldsymbol{\psi}^{(n-1)}$. Then, the original optimization problem (8) can be transformed into:

$$\max_{p_l} G_{t,1}(p_l) = \tilde{G}_{t,1}(p_l) + C_1, \tag{10}$$

$$\text{s.t.} \quad 0 \leq p_l - b_m \leq 2a_m P_S^{\max}, \tag{10a}$$

$$c_{a,2}^{t,1}\,(p_l - b_m) \leq \eta_a P_a^{max}, \tag{10b}$$

$$c_{h,4}^{t,1}\,(p_l - b_m) \leq \eta_h P_h^{max}, \tag{10c}$$

$$\eta_a E_a^{min} \leq c_{a,2}^{t,1} \nu_a^{(n-1)} (p_l - b_m) \leq \eta_a E_a^{max}, \tag{10d}$$

$$\eta_h E_h^{min} \leq c_{h,4}^{t,1} \mu_h^{(n-1)} (p_l - b_m) \leq \eta_h E_h^{max}, \tag{10e}$$

where

$$\begin{aligned} \tilde{G}_{t,1}(p_l) = &\sum_{a=1}^{A} c_{a,1}^{t,1} \log_2 \left[1 + c_{a,2}^{t,1}\,(p_l - b_m)\right] \\ &+ \sum_{h=1}^{H} c_{h,3}^{t,1} \log_2 \left[1 + c_{h,4}^{t,1}\,(p_l - b_m)\right] - c_5^{t,1} p_l (p_l - b_m), \end{aligned} \tag{11}$$

$$\boldsymbol{U}_L(p_l,\beta,\boldsymbol{\psi})=p_r\left\{\sum_{p=1}^{P}\gamma_p \mathrm{W}_p\theta_p+\sum_{a=1}^{A}\nu_a\kappa_a\log_2\left[1+\delta_a\frac{\beta(p_l-b_m)}{2\nu_a a_m}\right]+\sum_{h=1}^{H}\left[\gamma_h \mathrm{W}_h\tau_h+\mu_h\kappa_h\log_2\left(1+\delta_h\frac{(\beta-\tau_h)(p_l-b_m)}{2\mu_h a_m}\right)\right]\right\}-\frac{p_l\beta(p_l-b_m)}{2a_m}. \quad (7)$$

$$C_1=p_r\left(\sum_{p=1}^{P}\gamma_p W_p\theta_p^{(n-1)}+\sum_{h=1}^{H}\gamma_h W_h\tau_h^{(n-1)}\right)=const., \quad (12)$$

$c_{a,1}^{t,1}=p_r\nu_a^{(n-1)}\kappa_a$, $c_{a,2}^{t,1}=\frac{\delta_a\beta^{(n-1)}}{2\nu_a^{(n-1)}a_m}$, $c_{h,3}^{t,1}=p_r\mu_h^{(n-1)}\kappa_h$, $c_{h,4}^{t,1}=\frac{\delta_h\left(\beta^{(n-1)}-\tau_h^{(n-1)}\right)}{2\mu_h^{(n-1)}a_m}$, and $c_5^{t,1}=\frac{\beta^{(n-1)}}{2a_m}$.

Lemma 1. *The objective function $G_{t,1}$ is a concave function w.r.t. p_l satisfying the linear constraints in* (10a)-(10e)*, and the optimal solution for the single variable sub-problem* (10) *can be obtained by line search methods.*

Proof. The detailed proof is presented in [20]. □

B. Optimal Emitting Time of the PB

Similar to the sub-problem (10), the time constraints and transmission power constraint of the PB are always satisfied with the fixed $\{p_l^{(n)},\boldsymbol{\psi}^{(n-1)}\}$, thus they can be totally ignored. The optimal emitting time β of the PB in the n-th iteration can be obtained by solving the following sub-problem:

$$\max_{\beta} G_{t,2}(\beta)=\tilde{G}_{t,2}(\beta)+C_1, \quad (13)$$

$$\text{s.t.}\quad 0\le\beta\le 1, \quad (13a)$$

$$c_{a,2}^{t,2}\beta\le\eta_a P_a^{max}, \quad (13b)$$

$$c_{h,4}^{t,2}\left(\beta-\tau_h^{(n-1)}\right)\le\eta_h P_h^{max}, \quad (13c)$$

$$\eta_a E_a^{min}\le c_{a,2}^{t,2}\nu_a^{(n-1)}\beta\le\eta_a E_a^{max}, \quad (13d)$$

$$\eta_h E_h^{min}\le c_{h,4}^{t,2}\mu_h^{(n-1)}\left(\beta-\tau_h^{(n-1)}\right)\le\eta_h E_h^{max}, \quad (13e)$$

where

$$\tilde{G}_{t,2}(\beta)=\sum_{a=1}^{A}c_{a,1}^{t,2}\log_2\left(1+c_{a,2}^{t,2}\beta\right)+\sum_{h=1}^{H}c_{h,3}^{t,2}\log_2\left[1+c_{h,4}^{t,2}\left(\beta-\tau_h^{(n-1)}\right)\right]-c_5^{t,2}\beta, \quad (14)$$

$c_{a,1}^{t,2}=p_r\nu_a^{(n-1)}\kappa_a$, $c_{a,2}^{t,2}=\frac{\delta_a\left(p_l^{(n)}-b_m\right)}{2\nu_a^{(n-1)}a_m}$, $c_{h,3}^{t,2}=p_r\mu_h^{(n-1)}\kappa_h$, $c_{h,4}^{t,2}=\frac{\delta_h\left(p_l^{(n)}-b_m\right)}{2\mu_h^{(n-1)}a_m}$, and $c_5^{t,2}=\frac{p_l^{(n)}\left(p_l^{(n)}-b_m\right)}{2a_m}$.

Lemma 2. *The objective function $G_{t,2}$ is a concave function w.r.t. β satisfying the linear constraints in* (13a)-(13e)*, and the optimal solution for the single variable sub-problem* (13) *can be obtained by line search methods.*

Proof. The detailed proof is presented in [20]. □

C. Optimal Time Resource Allocation

In this subsection, we investigate the scheduling times $\boldsymbol{\psi}^{(n)}$ based on the given $\{p_l^{(n)},\beta^{(n)}\}$. The original optimization problem (8) is simplified into:

$$\max_{\boldsymbol{\psi}} G_{t,3}(\boldsymbol{\psi})=\tilde{G}_{t,3}(\boldsymbol{\psi})-C_2, \quad (15)$$

$$\text{s.t.}\ c_{a,1}^{t,3}\le\eta_a\nu_a P_a^{max}, \quad (15a)$$

$$c_{h,2}^{t,3}-c_{h,3}^{t,3}\tau_h\le\eta_h\mu_h P_h^{max}, \quad (15b)$$

$$\eta_h E_h^{min}\le c_{h,2}^{t,3}-c_{h,3}^{t,3}\tau_h\le\eta_h E_h^{max}, \quad (15c)$$

$$0\le\sum\nolimits_{p=1}^{P}\theta_p+\sum\nolimits_{h=1}^{H}\tau_h\le\beta^{(n)},\forall\theta_p,\forall\tau_h\ge 0, \quad (15d)$$

$$0\le\sum\nolimits_{a=1}^{A}\nu_a+\sum\nolimits_{h=1}^{H}\mu_h\le 1-\beta^{(n)},\forall\nu_a,\forall\mu_h\ge 0, \quad (15e)$$

where

$$\tilde{G}_{t,3}(\boldsymbol{\psi})=p_r\left\{\sum_{p=1}^{P}\gamma_p \mathrm{W}_p\theta_p+\sum_{a=1}^{A}\nu_a\kappa_a\log_2\left(1+\frac{c_{a,1}^{t,3}}{\nu_a}\right)+\sum_{h=1}^{H}\left[\gamma_h \mathrm{W}_\mathrm{h}\tau_h+\mu_h\kappa_h\log_2\left(1+\frac{c_{h,2}^{t,3}-\tau_h c_{h,3}^{t,3}}{\mu_h}\right)\right]\right\}, \quad (16)$$

$$C_2=\frac{p_l^{(n)}\beta^{(n)}\left(p_l^{(n)}-b_m\right)}{2a_m}=const., \quad (17)$$

$c_{a,1}^{t,3}=\frac{\delta_a\beta^{(n)}\left(p_l^{(n)}-b_m\right)}{2a_m}$, $c_{h,2}^{t,3}=\frac{\delta_h\beta^{(n)}\left(p_l^{(n)}-b_m\right)}{2a_m}$, and $c_{h,3}^{t,3}=\frac{\delta_h\left(p_l^{(n)}-b_m\right)}{2a_m}$. Note that, the energy constraints for AWPDs are removed because they always be satisfied with the fixed $\{p_l^{(n)},\beta^{(n)}\}$. To obtain the optimal solution for the sub-problem (15), we have the following Lemma 3.

Lemma 3. *The objective function $G_{t,3}$ is a concave function w.r.t. $\boldsymbol{\psi}$ satisfying the linear constraints in* (15a)-(15e)*, and the optimal solution for the sub-problem* (15) *can be obtained by the interior-point method.*

Proof. The detailed proof is presented in [20]. □

Then, the proposed iterative algorithm is summarized in the **Algorithm 1**. Its convergence is provided in the following Theorem.

Theorem 1. *The Algorithm 1 is guaranteed to converge to the local optimal solution of the ISP's maximization problem.*

Proof. The detailed proof is presented in [20]. □

Finally, a local SE of the proposed Stackelberg game can be obtained, formally stated in the following Theorem.

Theorem 2. *A local SE $(P_S^*,\hat{\boldsymbol{\chi}}^*)$ obtained by the closed-form solution of the ESP's maximization problem and the Theorem 1 satisfies the Definition 2.*

Proof. From the Theorem 1, we have the output $\hat{\boldsymbol{\chi}}^*$ of the **Algorithm 1** is a locally optimal solution of the problem (8). It means that $\boldsymbol{U}_L(\hat{\boldsymbol{\chi}}^*,P_S^*)\ge\boldsymbol{U}_L(\boldsymbol{\chi},P_S^*)$ in the neighborhood

Algorithm 1 The iterative algorithm to solve the non-convex optimization problem in (8).

Input: The previous output $\{{p_l}^{(n-1)}, \beta^{(n-1)}, \boldsymbol{\psi}^{(n-1)}\}$.
Initialize: $n = 1$, $\{{p_l}^{(0)}, \beta^{(0)}, \boldsymbol{\psi}^{(0)}\}$, tolerance $\xi > 0$.
Compute: the leader's utility $\boldsymbol{U}_L\left({p_l}^{(0)}, \beta^{(0)}, \boldsymbol{\psi}^{(0)}\right)$.
Repeat:
  Obtain ${p_l}^{(n)}$ from $\{{p_l}^{(n-1)}, \beta^{(n-1)}, \boldsymbol{\psi}^{(n-1)}\}$ by solving (10);
  Derive $\beta^{(n)}$ with fixed $\{{p_l}^{(n)}, \boldsymbol{\psi}^{(n-1)}\}$ by solving (13);
  For given $\{{p_l}^{(n)}, \beta^{(n)}\}$, $\boldsymbol{\psi}^{(n)}$ is obtained by solving (15);
  If:
    $\left|\boldsymbol{U}_L\left({p_l}^{(n)}, \beta^{(n)}, \boldsymbol{\psi}^{(n)}\right) - \boldsymbol{U}_L\left({p_l}^{(n-1)}, \beta^{(n-1)}, \boldsymbol{\psi}^{(n-1)}\right)\right| < \xi$;
  Then:
    Set $\{\hat{p}_l^*, \hat{\beta}^*, \hat{\boldsymbol{\psi}}^*\} = \{{p_l}^{(n)}, \beta^{(n)}, \boldsymbol{\psi}^{(n)}\}$ and terminate.
  Otherwise:
    Update $n \leftarrow n + 1$ and continue.
Output: The optimal solution $\hat{\boldsymbol{\chi}}^* = \{\hat{p}_l^*, \hat{\beta}^*, \hat{\boldsymbol{\psi}}^*\}$.

of $\hat{\boldsymbol{\chi}}^*$. Thus, the pair $(P_S^*, \hat{\boldsymbol{\chi}}^*)$ is a local SE of the proposed Stackelberg game that satisfying the Definition 2. □

V. Numerical Results

In this section, numerical simulations are provided to evaluate the performance of the proposed scheme which jointly controls transmission power of the PB and schedules time resources for the IoT devices. We consider the carrier frequency of RF signals at 2.4 GHz. The bandwidth of the RF signals and the antenna gain of the PB are 10 MHz and 6 dBi, respectively. The IoT devices (i.e., AWPDs and HWPDs) have the antenna gains of 6 dBi [21]. Unless otherwise specified, the default backscatter rate of backscatter devices is set at 10 kpbs. In our setup, both the AWPDs and HWPDs have the energy harvesting and data transmission efficiency coefficients of $\varphi = 0.6$ and $\phi = 0.5$, respectively. For the benchmark, other conventional methods, i.e., the BBCM, HTTCM, and TDMA mechanism are utilized to compare with the proposed scheme. It is worth noting that, all IoT devices are allocated with identical time resources in the TDMA mechanism. Besides, the BBCM only requires the PB to transmit its RF signals in the whole time-frame with the lower and fixed transmission power (i.e., 13 dBm) [10].

A. Identical Number of Devices for each IoT Devices' Set

We first evaluate the performance of the proposed scheme under the setting that the number of devices in each IoT devices' type are equal, (i.e., $N = 10$). In Fig. 2, we show the variation of the leader's payoff (i.e., the ISP) as the backscatter rate increases in the range of 5 kbps to 50 kbps. In general, the utilities of the leader obtained by the proposed scheme, BBCM, and TDMA increase as the backscatter rate increases. Considering the backscatter rate under 45 kbps, the proposed scheme attempts to schedule more time resources for the IoT devices to transmit data actively, and thus the total profit corresponding with R^{st} is higher than R^{bb} as illustrated in Fig. 2. Nonetheless, for a higher backscatter rate (i.e., more than 45 kbps), the benefit contributed by the backscatter communications is increased, thus all IoT devices with backscattering circuits are imposed on using the BBCM only to achieve the better utility greedily. Note that, in such a circumstance, the PB will transmit its signals at 13 dBm. This result exposes a noticeable strategy for the ISP. By contrast, due to the equal allocation of time resources among all IoT device types in the TDMA mechanism, the leader's payoff increases linearly together with the backscatter rate.

The backscatter rate is now set by default (i.e., 10 kbps) under different numbers of devices for all three IoT devices' sets $(i.e., N = \{5, 7, 9\})$. Fig. 3 demonstrates the relation between the emitting time of the PB and the energy price offered by the ISP for backscattering signal and harvesting energy. It can be seen that the offered price is maximum at 10 (price unit) when the emitting time of the PB is short (i.e., smaller than 0.25). The reason is that if the PB transmits its signal in a short time, it must emit at high power to guarantee that the AWPDs and HWPDs can harvest enough energy for their operations in the idle period of the PB. When the emitting time of the PB is long, the IoT devices only need a lower transmission power from the PB to maximize its profit. For $N = 9$, the offered price p_l will be smaller than other cases $(i.e., N = \{5, 7\})$ when the emitting time of PB is higher than 0.35. It is due to the fact that the more AWPDs and HWPDs, the more profit achieved by them at the same emitting time. A similar result can be obtained when the emitting time is higher than 0.475, i.e., the offered price p_l for the case of $N = 7$ is smaller than the case of $N = 5$.

As shown in Fig. 4, the computing efficiency of the proposed BCD method in the **Algorithm 1** is investigated by varying the number of devices for all three IoT devices' sets $(i.e., N = \{5, 7, 9\})$. The runtime of the proposed algorithm increases according to the number of devices. For the case of 9 devices, it only takes a maximum of less than 6 seconds and an average of less than 4 seconds to converge to the SE point after 1000 tests. Whilst the average runtime in the cases of $N = 5$ and $N = 7$ are 2.6 and 3.1 seconds, respectively.

B. Different Number of Devices for each IoT Devices' Set

We then investigate the leader's payoff of the proposed scheme by altering the number of devices for one type from 2 to 20, while keeping these figures for other types fixed at 10. As shown in Fig. 5, the proposed scheme achieves the highest profit compared with the others in the first two cases (Fig. 5(a), Fig. 5(b)) when the number of IoT devices is higher than 6 for HWPDs, and 4 for AWPDs, respectively. The reason is that when the numbers of HWPDs and AWPDs are small, more time is allocated for PWPDs in the emitting period which will boost the profit of the TDMA mechanism compared to the proposed scheme. When these numbers increase, then the proposed scheme can outperform the TDMA mechanism. However, as the numbers of HWPDs and AWPDs are higher than 10, there is no more profit added to the proposed scheme, and HTTCM as shown in Fig. 5(a) and Fig. 5(b) because the power constraints of IoT devices (i.e., AWPDs and HWPDs) are violated. In addition, as illustrated in Fig. 5(c), the increase in the number of PWPDs causes no impact on the profit of the proposed scheme due to the low level of backscatter rate. By contrast, due to sharing the time resources for PWPDs, the profit of the TDMA mechanism reduces linearly.

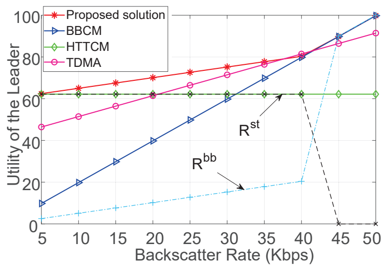

Fig. 2: Leader's payoff vs backscatter rate.

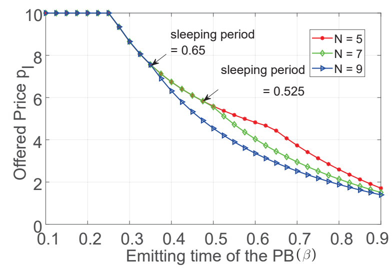

Fig. 3: Offered price vs emitting time of the PB.

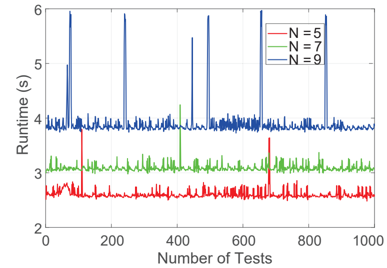

Fig. 4: Runtime of the proposed iterative algorithm.

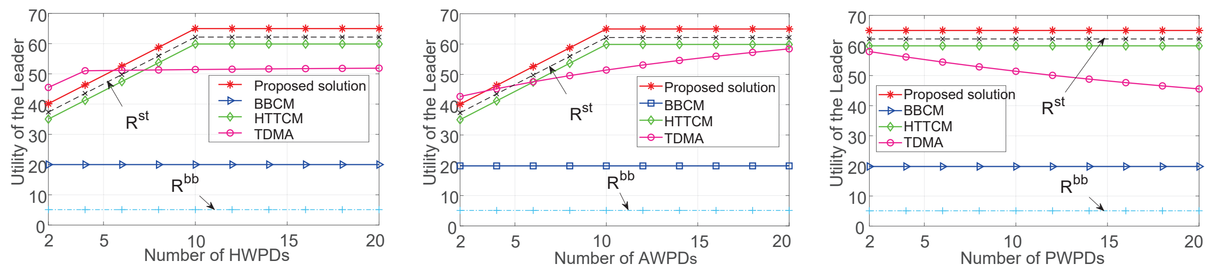

(a) (b) (c)

Fig. 5: Leader's payoff under different numbers of (a) HWPDs, (b) AWPDs, and (c) PWPDs.

VI. Summary

In this paper, we have studied the Stackelberg game to maximize the profits of both service providers in heterogeneous IoT wireless-powered communication networks. Then, the local *Stackelberg equilibrium* presented the proper price for the energy service, the optimal emitting time of the PB, and the optimal scheduling times for the IoT service has been obtained via the closed-form and the proposed iterative algorithm that exploits the BCD technique. Numerical analyses have shown the fast convergence and computing efficiency of the proposed iterative algorithm. Simulation results have shown that the achievable profit of the proposed scheme always outperforms other baseline methods.

References

[1] A. A. Fuqaha et al., "Internet of Things: A Survey on Enabling Technologies, Protocols, and Applications," *IEEE Commun. Surv. & Tut.*, vol. 17, no. 4, pp. 2347-2376, June 2015.

[2] D. W. K. Ng et al., "The Era of Wireless Information and Power Transfer," in *Wireless Information and Power Transfer: Theory and Practice,* Wiley, pp.1-16, 2019.

[3] S. Gong et al., "Backscatter Relay Communications Powered by Wireless Energy Beamforming," *IEEE Trans. Commun.,* vol. 66, no. 7, pp. 3187-3200, July 2018.

[4] D. T. Hoang et al.,"Overlay RF-powered backscatter cognitive radio networks: A game theoretic approach," in *IEEE Inter. Conf. on Commun.,* Paris, May 2017, pp. 1-6.

[5] W. Wang et al., "Stackelberg Game for Distributed Time Scheduling in RF-Powered Backscatter Cognitive Radio Networks," *IEEE Trans. on Wireless Commun.*, vol. 17, no. 8, pp. 5606-5622, Aug. 2018.

[6] H. Ju and R. Zhang, "Throughput maximization in wireless powered communication networks," *IEEE Trans. Wireless Commun.*, vol. 13, no. 1, pp. 418-428, Jan. 2014.

[7] N. Van Huynh et al., "Ambient Backscatter Communications: A Contemporary Survey," *IEEE Commun Surv. & Tut.,* vol. 20, no. 4, pp. 2889-2922, May 2018.

[8] A. M. Rad et al., "Autonomous demand-side management based on game-theoretic energy consumption scheduling for the future smart grid," *IEEE Trans. Smart Grid*, vol. 1, no. 3, pp. 320-331, Dec. 2010.

[9] P. Tseng, "Convergence of a block coordinate descent method for nondifferentiable minimization," *Jour. Optim. Theory Appl.*, vol. 109, no. 3, pp. 475–494, June 2001.

[10] N. F. Hilliard, P. N. Alevizos and A. Bletsas,"Coherent Detection and Channel Coding for Bistatic Scatter Radio Sensor Networking," *IEEE Trans. Commun.,* vol. 63, no. 5, pp. 1798-1810, May 2015.

[11] C. A. Balanis, *Antenna Theory: Analysis and Design*. NY, Wiley, 2012.

[12] D. Fudenberg, J. Tirole, *Game Theory*, MIT Press, 1991.

[13] FCC Rules for RF devices, part 15, Oct 2018. Accessed on May 12, 2020. [Online] Available: http://afar.net/tutorials/fcc-rules/.

[14] P. Siyari, M. Krunz, and D. N. Nguyen, "Friendly Jamming in a MIMO Wiretap Interference Network: A Nonconvex Game Approach," *IEEE J. Sel. Areas Commun.,* vol. 35, no. 3, pp. 601-614, Mar. 2017.

[15] X. Huang, B. Beferull-Lozano, and C. Botella, "Quasi-Nash equilibria for non-convex distributed power allocation games in cognitive radios," *IEEE Trans. Wireless Commun.,* vol. 12, no. 7, pp. 3326–3337, Jul. 2013.

[16] G. Scutari and J. S. Pang, "Joint sensing and power allocation in nonconvex cognitive radio games: Nash equilibria and distributed algorithms," *IEEE Trans. Wireless Commun.,* vol. 59, no. 7, pp. 4626–4661, Jul. 2013.

[17] F. Facchinei and J. Pang, *Finite-Dimensional Variational Inequalities Complementarity Problems.* New York, NY, USA: Springer, 2007.

[18] C. Daskalakis and I. Panageas, "The limit points of (optimistic) gradient descent in min-max optimization," in *Advances in Neural Information Processing Systems*, Dec. 2018, pp. 9256–9266.

[19] E. Mazumdar and L. J. Ratliff, "On the convergence of gradient-based learning in continuous games" arXiv preprint arXiv:1804.05464, 2018.

[20] Ngoc-Tan Nguyen et al., "Time Scheduling and Energy Trading for Heterogeneous Wireless-Powered and Backscattering-based IoT Networks," *Submitted to TWC*, 2020. [Online]. Available: https://arxiv.org/abs/2005.14573.

[21] D. Y. Kim and D. I. Kim, "Reverse-link interrogation range of a UHF MIMO-RFID system in Nakagami-m fading channels," *IEEE Trans. Indus. Electron.*, vol. 57, no. 4, pp. 1468-1477, Apr. 2010.